Graphene Growth via Carburization of Stainless Steel and Application in Energy Storage

Hemtej Gullapalli, Arava Leela Mohana Reddy, Stephen Kilpatrick, Madan Dubey, and Pulickel M. Ajayan*

A modified version of the carburization process, a widely established technique used in the steel industry for case hardening of components, is used for the growth of graphene on stainless steel. Controlled growth of high-quality single- and few-layered graphene on stainless steel (SS) foils through a liquid-phase chemical vapor deposition (CVD) technique is reported. Reversible Li intercalation in these graphene-on-SS structures is demonstrated, where graphene and SS act as electrode and current collector, respectively, providing very good electrical contact. Direct growth of an active electrode material, such as graphene, on current-collector substrates makes this a feasible and efficient process for developing thin-film battery devices.

1. Introduction

Carburization is a well known process, developed decades ago in the steel industry, and is used to case-harden steel using a low quantity of carbon. In this process, steel is introduced to a carbon-rich environment at elevated temperatures for a certain amount of time and then quenched so that the carbon is locked in the crystal structure. It will be of fundamental interest if the dynamics of this carbon-atom diffusion and kinetics can be slightly modified in order to achieve few-layers-thick graphene on stainless steel (SS) substrates. Though the carburization process is similar to the chemical vapor deposition (CVD) technique, which is generally used for growth of graphene on
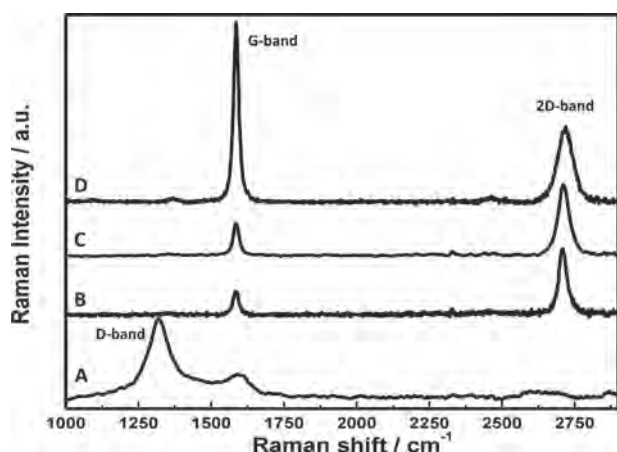
H. Gullapalli, Dr. A. L. M. Reddy
Department of Mechanical Engineering and Materials Science
Rice University
Houston, TX 77005, USA
S. Kilpatrick, Dr. M. Dubey
US Army Research Laboratory
2800 Powder Mill Road, Adelphi, MD 20783, USA
Prof. P. M. Ajayan
Department of Mechanical Engineering
and Materials Science
Rice University
Houston, TX 77005, USA
E-mail: ajayan@rice.edu

metals such as copper, the duration of heating, diffusion, and cooling steps are the key in determining the carbon structure that finally forms on the substrate.[1] In this Full Paper, we report that a slightly modified carburization process can indeed result in controlled growth of graphene layers on SS substrates.

Graphene has been the focus of significant attention recently due to its unique physical and electrical properties.[2] Recently, graphene has also been considered as an efficient candidate for the electrode material in Li-ion batteries due to its high electrical conductivity, high surface area, and broad electrochemical window.[3–8] For the initial studies on graphene for battery applications, the primary synthesis method was exfoliation of graphite or reduced graphite oxide, resulting in micrometer-size graphene flakes. Poor adherence between the individual flakes and the substrate results in a poor electrical contact, thereby reducing the performance of such energy-storage devices. In order to address this conductivity issue, there is a need for direct fabrication of graphene electrode materials on chemically and mechanically stable conducting current collectors. Growth of high-quality few-layer graphene on various metallic substrates has been extensively studied and well documented.[9–12] However, these metallic substrates are not viable for use in lithium-ion batteries and would require the transfer of graphene on to current collectors, such as stainless steel. By directly growing graphene on stainless steel, these carbon layers can be directly used in Li-ion battery applications. Moreover, since stainless steel is a chemically and thermally stable material, compared to pure metals such

1. REPORT DATE **2011**	2. REPORT TYPE	3. DATES COVERED **00-00-2011 to 00-00-2011**

4. TITLE AND SUBTITLE	5a. CONTRACT NUMBER
Graphene Growth via Carburization of Stainless Steel and Application in Energy Storage	5b. GRANT NUMBER
	5c. PROGRAM ELEMENT NUMBER
6. AUTHOR(S)	5d. PROJECT NUMBER
	5e. TASK NUMBER
	5f. WORK UNIT NUMBER

7. PERFORMING ORGANIZATION NAME(S) AND ADDRESS(ES) **Rice University,Department of Mechanical Engineering and Materials Science,6100 S. Main Street,Houston,TX,77005**	8. PERFORMING ORGANIZATION REPORT NUMBER

9. SPONSORING/MONITORING AGENCY NAME(S) AND ADDRESS(ES)	10. SPONSOR/MONITOR'S ACRONYM(S)
	11. SPONSOR/MONITOR'S REPORT NUMBER(S)

12. DISTRIBUTION/AVAILABILITY STATEMENT **Approved for public release; distribution unlimited**

13. SUPPLEMENTARY NOTES

14. ABSTRACT

15. SUBJECT TERMS

16. SECURITY CLASSIFICATION OF:			17. LIMITATION OF ABSTRACT	18. NUMBER OF PAGES	19a. NAME OF RESPONSIBLE PERSON
a. REPORT **unclassified**	b. ABSTRACT **unclassified**	c. THIS PAGE **unclassified**	**Same as Report (SAR)**	**4**	

Figure 1. Raman spectra of SS substrates after carbon heat treatment and being A) quenched, resulting in carburized steel with a highly defective graphitized structure, B) cooled at a rate of 15 °C s⁻¹, resulting in one-layer graphene, C) cooled at a rate of 2 °C s⁻¹, resulting in 1–2-layer graphene, and D) cooled at a rate of 0.7 °C s⁻¹, forming more than three layers of graphene.

as copper and nickel, this method opens up greater possibilities where the graphene can be further modified physically or functionally without affecting the underlying substrate.

2. Results and Discussion

Commercially available carburized steel was examined by Raman spectroscopy (**Figure 1**A) to determine the structure of carbon on its surface and was found to have prominent disorder-induced 1D band centered at 1368 cm⁻¹ and a very low intense symmetry-allowed graphite band (G-band) at ≈1585 cm⁻¹. As is evident from this, the carburization process yields a structure resembling discontinuous graphitic domains. The spectrum demonstrates that commercial carburization does not form graphene on the surfaces but the process creates disordered graphitic carbon. In this case, carburizing involves heating steel in a carbon atmosphere to around 1000 °C and holding the temperature for a while. The sample is then quickly quenched to low temperature. Due to this quenching process, the carbon is not allowed to resurface and gets trapped in the bulk of the lattice. The very minute quantity of carbon present on the surface graphitizes and results in such a structure.

However, we show that small changes in the process conditions yields graphene on similar steel surfaces. By keeping the heat-treatment conditions similar to carburization, except for the cooling rate, carbon deposition has been carried out on SS (grade 304 from Alfa Aser) foil using liquid-precursor chemical vapor deposition (CVD). Figure 1B–D shows the Raman spectra of samples cooled from 950 to 800 °C at cooling rates of 15, 2, and 0.7 °C s⁻¹, respectively. The number of layers present is estimated by comparing the intensities of the G peak at ≈1585 cm⁻¹ and the 2D peak at ≈2700 cm⁻¹.[13] From the intensity ratios of the 2D and G bands, it is clear that the sample in Figure 1B has one layer of graphene, Figure 1C has 1–2 layers of graphene, and the sample in Figure 1D contains 3 or more layers of graphene. Moreover, the D peak at 1368 cm⁻¹ is negligible in these samples, confirming that there

are significantly less defects in the graphene. Our observations reveal that the quenching/cooling time used in the CVD process plays a crucial role and dictates the morphology of the carbon growth on steel. In commercial carburization, due to quick quenching, the carbon atoms do not have enough time to leave the lattice and hence are trapped in it, thereby hardening the steel, whereas, in the case of a slow cooling process, the carbon atoms will have enough time to diffuse out of the lattice and crystallize on the surface, resulting in few graphitic layers. The speed of cooling dictates the number of layers of graphene, whereas the duration of carbon-source flow is found to have little influence. However, a significantly shorter time of exposure resulted in discontinuous graphene growth. A control experiment done with an exposure time of 3 min resulted in defective 1–2-layer graphene, while a long 40-min exposure followed by similar cooling yielded high-quality 1–2-layer graphene, as shown in Figure S1 in the Supporting Information. This is mainly because the solubility of carbon in austenitic steel is very minimal at 950 °C and the graphene growth is believed to happen only when the sample is cooling down. The graphene films are continuous over a large area with no visible defects and few wrinkles, as observed in the scanning electron microscopy (SEM) images shown in **Figure 2**A–C. Figure 2D,E show high-resolution transmission electron microscopy (HRTEM) images of the graphene with the electron diffraction pattern in the inset. We have observed three layers in numerous flakes, confirming continuity in the samples.

Lithium-ion rechargeable batteries are based on carbon electrodes, wherein metallic lithium is replaced by a carbon
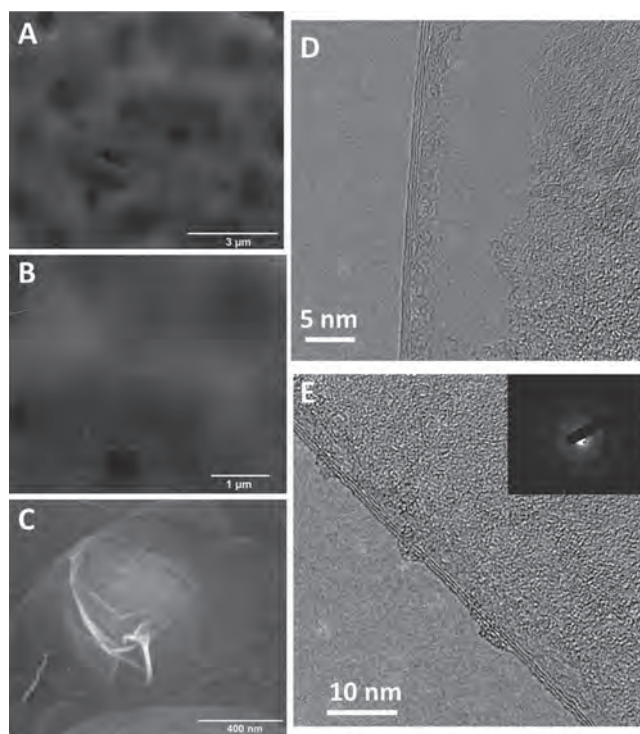
Figure 2. A–C) SEM images at various magnifications of the graphene on the SS foil grown by liquid-precursor-based CVD. D,E) HRTEM images of three-layered graphene with the diffraction spectra in the inset of (E).

host structure that can reversibly intercalate and deintercalate lithium ions at low electrochemical potential.[14] There have been several efforts to increase the energy density and specific capacity of these cells by using different types of carbon structures and their composites.[15–19] The applicability of the as-grown graphene electrodes for Li-ion batteries is tested by constructing a Li half cell using 3-layered graphene on stainless steel as the working electrode and Li foil as the counter and reference electrode. Galvanostatic charge/discharge measurements conducted at a constant current of 10 μA cm^{-2} between 3.2 and 0.02 V are shown in **Figure 3**A. The first cycle showed a discharge capacity of ≈0.2 mA h cm^{-2} with a large plateau at about 0.7 V. Considerable loss in capacity was observed in the second cycle (≈0.15 mA h cm^{-2}) due to the solid electrolyte interface (SEI) formation, which is very commonly observed in carbon-based electrodes. The plateau at 0.7 V in the first discharge curve can be attributed

to the formation of an SEI film on the surface of graphene associated with electrolyte decomposition and the formation of lithium–organic compounds.[20,21] In the subsequent cycles, the discharge plateau disappeared and a reversible capacity of 0.05 mA h cm^{-2} was observed after 50 cycles of charge/discharge (Figure 3B). This is comparable with previously reported values of carbon-based thin-film electrodes and also with our previous work on N-doped graphene electrodes grown on Cu substrates.[22,8] After the first cycle, the Coulombic efficiency remained very stable throughout subsequent cycles, indicating that the formed surface film remained intact.

Further, as the electrical contact between the electrode and the current collector plays an important role in determining the power density of a Li-ion battery, the performance of the graphene on SS when cycled at higher current rates is also analyzed through galvanostatic charge/discharge experiments. **Figure 4** shows the discharge capacity of the graphene electrode under various current rates. The electrode was initially cycled for five cycles at current rate of 2 μA cm^{-2}, during which the nominal capacity of ≈0.05 mA h cm^{-2} was observed. The current rate was then increased in steps for every five cycles, during which the graphene electrode is found to show stable performance. The electrode could retain ≈75% of the nominal capacity, even at higher rates. Upon reducing the current rate back to 2 μA cm^{-2}, the battery had regained its nominal capacity (≈0.05 mA h cm^{-2}), which clearly indicates that the electrode could withstand the high current rates.

3. Conclusion

In summary, we have demonstrated a facile and scalable method for the controlled growth of graphene layers on stainless steel substrates. Surprisingly, it is seen that good quality graphene can be grown on stainless steel by a
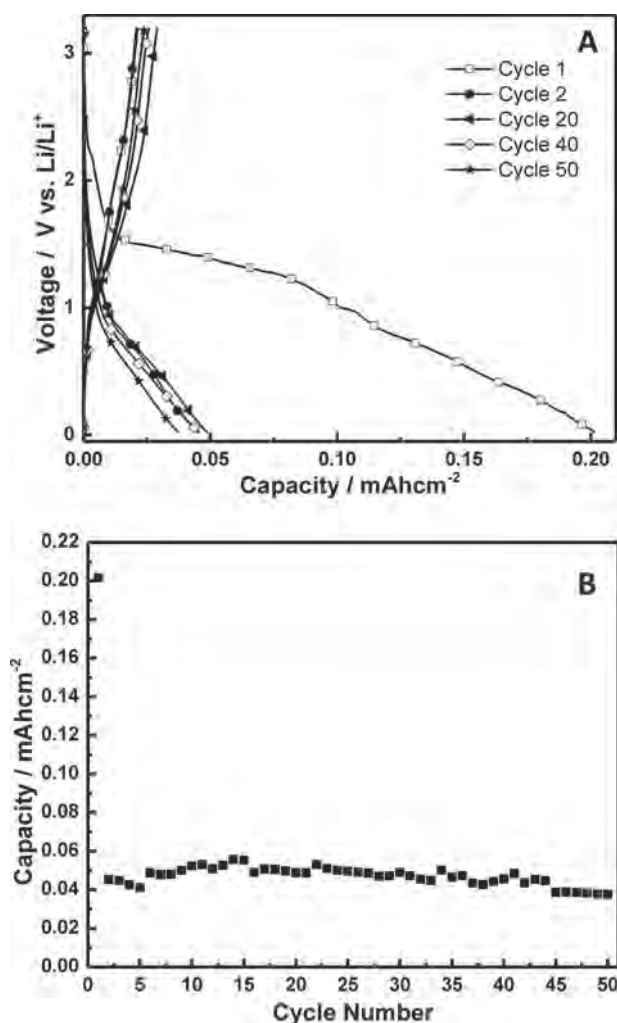
Figure 3. A) Charge/discharge voltage profiles for a 3-layered graphene electrode galvanostatically cycled at a rate of 5 μA cm^{-2} between 3.2 and 0.02 V versus Li/Li+. B) Variation in discharge capacity versus cycle number for the 3-layered graphene cycled at a rate of 5 μA g^{-1} between 3.2 and 0.02 V versus Li/Li+ in a 1 M solution of LiPF$_6$ in a 1:1 (v/v) mixture of ethylene carbonate (EC) and dimethyl carbonate (DMC) as the electrolyte.
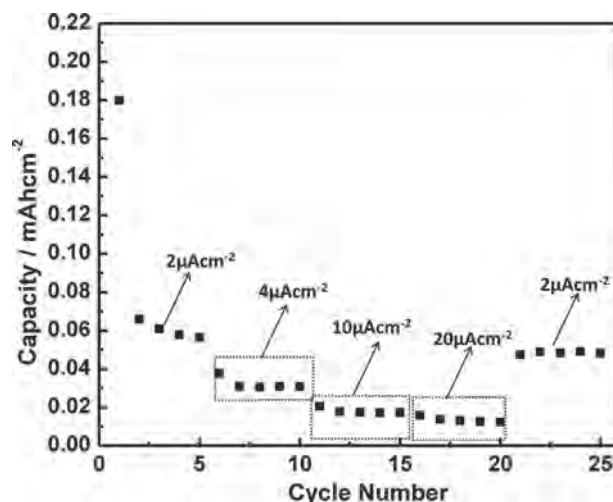
Figure 4. Rate-capability studies of graphene directly grown on SS substrates. Discharge capacity versus cycle number for various current rates. Good capacity retention is observed for high current rates and the nominal capacity is regained upon returning to lower current rates.

process similar to carburization, a process used for decades in steel industry. It is seen that the cooling rate of the sample after carbon-source exposure at high temperature controls the morphology of carbon growth on SS substrates. Good electrochemical properties and stability over Li-ion charge/discharge cycles make directly grown graphene on an SS current collector a promising candidate for ultrathin Li-ion batteries.

4. Experimental Section

Stainless steel foil (0.25-mm thick, type 304, from Alfa Aser) was inserted into the quartz tube (50-mm diameter × 4-foot length) of a CVD furnace equipped with a vacuum pump. The tube was first evacuated by pumping down to a base pressure of 0.2 mTorr and then heated to 950 °C with Ar/H flowing at a pressure of 5−9 torr. Once the desired temperature was reached, Ar/H was stopped and hexane vapor was passed for 6−8 min at a pressure of 0.5 Torr. The furnace was then cooled with hexane flow until 800 °C and then with Ar/H flow. For faster cooling rates, the furnace was opened partially or fully while cooling.

Raman measurements were performed using a Renishaw spectrometer with a 514-nm laser and a 50× objective. A sample for TEM was obtained by slightly etching steel using 10% nitric acid in ethanol for 30 min, followed by sonication in distilled water. The solution was then dropped on to a holey carbon-coated copper TEM grid.

Electrochemical measurements were carried using a Swagelok-type cell with directly grown graphene on an SS current collector as the working electrode, lithium metal as the counter/reference electrode, a glass microfiber filter separator, and 1 M $LiPF_6$ electrolyte solution dissolved in a mixture of ethylene carbonate (EC) and dimethyl carbonate (DMC) (1:1 v/v). The cells were assembled in an argon-filled glove box. Galvanostatic charge/discharge cycles were tested using an ARBIN BT 2010 battery analyzer at a constant current rate of 10 μA cm^{-2} between 3.2 and 0.02 V versus Li/Li$^+$ at room temperature.

Supporting Information

Supporting Information is available from the Wiley Online Library or from the author.

[1] H. Surm, O. Kessler, F. Hoffmann, P. Mayr, *Adv. Eng. Mater.* **2000**, *2*, 814−818.
[2] A. K. Geim, K. S. Novoselov, *Nat. Mater.* **2007**, *6*, 183−191.
[3] D. Wang, D. Choi, J. Li, Z. Yang, Z. Nie, R. Kou, D. Hu, C. Wang, L. V. Saraf, J. Zhang, I. A. Aksay, J. Liu, *ACS Nano* **2009**, *3*, 907−914.
[4] C. Wang, D. Li, C. O. Too, G. G. Wallace, *Chem. Mater.* **2009**, *21*, 2604−2606.
[5] S. Paek, E. Yoo, I. Honma, *Nano Lett.* **2009**, *9*, 72−75.
[6] E. Yoo, J. Kim, E. Hosono, H. Zhou, T. Kudo, I. Honma, *Nano Lett.* **2008**, *8*, 2277−2282.
[7] F. Campana, R. Kotz, J. Vetter, P. Novak, H. Siegenthaler, *Electrochem. Commun.* **2005**, *7*, 107−112.
[8] A. L. M. Reddy, A. Srivastava, S. R. Gowda, H. Gullapalli, M. Dubey, P. M. Ajayan, *ACS Nano* **2010**, *4*, 6337−6342.
[9] X. Li, W. Cai, J. An, S. Kim, J. Nah, D. Yang, R. Piner, A. Velamakanni, I. Jung, E. Tutuc, S. K. Banerjee, L. Colombo, R. S. Ruoff, *Science* **2009**, *324*, 1312−1314.
[10] L. Ci, L. Song, C. Jin, D. Jariwala, D. Wu, Y. Li, A. Srivastava, Z. F. Wang, K. Storr, L. Balicas, F. Liu, P. M. Ajayan, *Nat. Mater.* **2010**, *9*, 430−435.
[11] K. S. Kim, Y. Zhao, H. Jang, S. Y. Lee, J. M. Kim, K. S. Kim, J. Ahn, P. Kim, J. Choi, B. H. Hong, *Nature* **2009**, *457*, 706−710.
[12] A. Srivastava, C. Galande, L. Ci, L. Song, C. Rai, D. Jariwala, K. F. Kelly, P. M. Ajayan, *Chem. Mater.* **2010**, *22*, 3457−3461.
[13] A. C. Ferrari, J. C. Meyer, V. Scardaci, C. Casiraghi, M. Lazzeri, F. Mauri, S. Piscanec, D. Jiang, K. S. Novoselov, S. Roth, A. K. Geim, *Phys. Rev. Lett.* **2006**, *97*.
[14] T. Nagaura, K. Tozawa, *Prog. Batteries Sol. Cells* **1990**, *9*, 209.
[15] J. Dahn, A. Sleigh, H. Shi, J. Reimers, Q. Zhong, B. Way, *Electrochim. Acta* **1993**, *38*, 1179−1191.
[16] A. Yoshino, K. Sanechika, T. Nakajima, *US Patent #4668595*, **1987**.
[17] J. Dahn, R. Fong, M. Spoon, *Phys. Rev. B* **1990**, *42*, 6424−6432.
[18] A. L. M. Reddy, M. M. Shaijumon, S. R. Gowda, P. M. Ajayan, *Nano Lett.* **2009**, *9*, 1002−1006.
[19] R. Fong, U. von Sacken, J. R. Dahn, *J. Electrochem. Soc.* **1990**, *137*, 2009−2013.
[20] D. Aurbach, Y. Ein-Eli, *J. Electrochem. Soc.* **1995**, *142*, 1746−1752.
[21] E. Frackowiak, *Carbon* **1999**, *37*, 61−69.
[22] C. Li, Q. Sun, G. Jiang, Z. Fu, B. Wang, *J. Phys. Chem. C* **2008**, *112*, 13782−13788.